ACS OMEGA

http://pubs.acs.org/journal/acsodf

Article

Facile Multicomponent Synthesis, Computational, and Docking Studies of Spiroindoloquinazoline Compounds

Surya Cholayil Palapetta, Harichandran Gurusamy,* Sarojinidevi Krishnan, and Shanmugam Ponnusamy

Cite This: *ACS Omega* 2022, 7, 7874−7884

Read Online

ACCESS | Metrics & More | Article Recommendations | Supporting Information

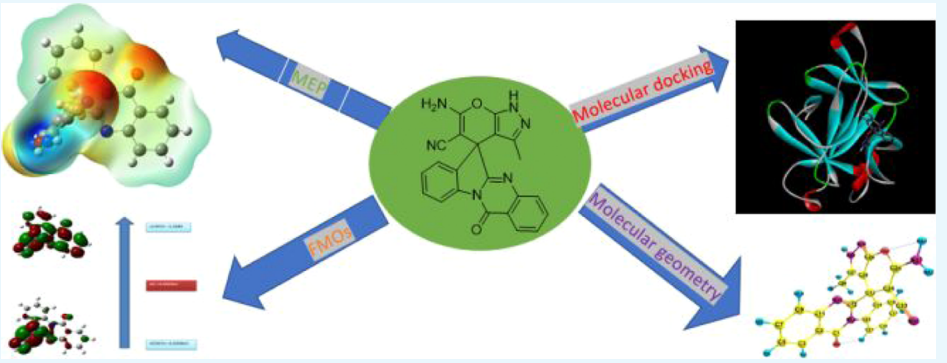

ABSTRACT: Synthesis of spiroindoloquinazolines via one-pot three-component condensation reactions of tryptanthrin, malononitrile or ethylcyanoacetate, and nucleophiles was carried out in MeOH using triethylamine as the base catalyst under reflux conditions. This method has the advantages of short reaction time, excellent yields, and an easy work-up procedure. The structural properties of the compound **4c** {2-amino-6-methyl-spiro-[12*H*]Indolo(2,1-*b*)quinazoline-12-one]12′,4-pyrano(2,3-*c*)pyrazole]-3-carbonitrile} and the obtained crystal were analyzed by the DFT theoretical calculation method, using the B3LYP 6-311G(d,p) basis set and were found to be in agreement with the experimental results. The importance of biological application and drug design of the same compound was verified by molecular docking studies.

INTRODUCTION

Synthesis of complex organic molecules by conventional methods involves a large number of synthetic operations, extraction, and purification processes. A conventional method leads not only to inefficient synthesis but also to the production of a large amount of waste. Multicomponent reactions (MCRs) play an essential task in organic synthesis, since they normally take place in one pot, afford high atom economy and selectivity, and offer the possibility of diversifying products by varying the different reactants.[1] MCRs are performed without any isolation of the intermediates, thus saving energy and raw materials and reducing the duration of the reaction.[2] Hence, the proposal of new MCRs has received great attention from research groups working in the fields of medicinal chemistry, drug discovery, and materials science. In addition, improvements in the already known MCRs are also of substantial interest in current organic synthesis. Quinoxalines are an important class of benzoheterocyclic derivatives that find pharmacological applications as an antidepressant, antifungal, antibacterial, and antitumor agents.[3−6] Tryptanthrin (indolo[2,1-*b*]quinazolin-6,12-dione) and its derivatives are indoloquinazoline alkaloids found in many kinds of plants and have various biological activities such as antiinflammatory, immunomodulatory, and antitumor activities.[7,8] In addition, these compounds inhibit the activity of microorganisms and parasites.[9,10] In recent years, tryptanthrin has received much attention as an anticancer agent.[11] Tryptanthrin was recognized with outstanding cytotoxicity against human breast carcinoma (MCF-7), lung carcinoma (NCI-H460), and central nervous system carcinoma (SF-268) cell lines. On the other hand, pyrans are an important building block unit and are present in many plants.[12] Pyrans and their derivatives have received a considerable interest because of biological properties such as anticancer activity and diuretic, spasmolytic, and hypertensive agents.[13,14] Interestingly, when the quinazoline ring of the spiroquinazoline system with pyrans is joined to a heterocyclic structure with a spiro carbon at the C-12 site, the resulting compounds show a wide spectrum of pharmacological activities. Also, the oxadiazoline structure has many pharmacological activities. The oxadiazoline moiety at C-12 of

Received: December 1, 2021
Accepted: February 11, 2022
Published: February 24, 2022

Scheme 1. Synthesis of Spiroindoloquinazoline Compounds

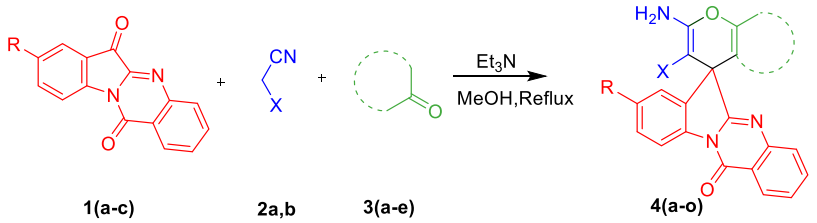

Table 1. Optimization of Reaction for the Synthesis of 4a

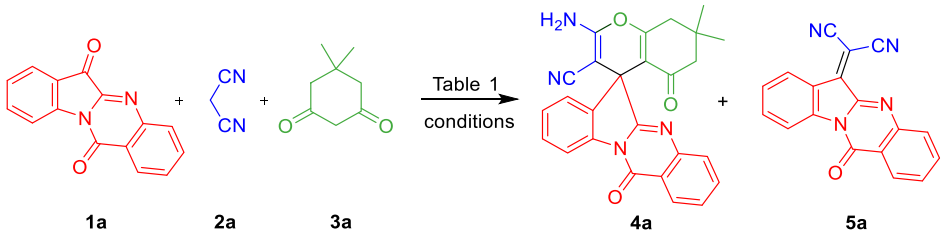

					product yield (%)	
entry	catalyst (equiv)	solvent	temp (°C)	time (min)	**4a**	**5a**
1			reflux	120		92
2		MeOH	reflux	120		93
3	K10-Clay(1 equiv)	MeOH	reflux	120		94
4	Iodine (1 equiv)	MeOH	reflux	120		93
5	IRA-400 Cl (1 equiv)	MeOH	reflux	120		92
6	**Et_3N** (1 equiv)	**MeOH**	**reflux**	**60**	**85**	**8**
7	Et_3N (1 equiv)	MeOH	RT	60	40	17
8	Et_3N (2 equiv)	MeOH	reflux	60	85	10
9	Et_3N (0.5 equiv)	MeOH	reflux	60	63	19
10	Et_3N (1 equiv)	DMSO	reflux	60	80	10
11	Et_3N (1 equiv)	MeCN	reflux	60	Trace	52
12	Et_3N (1 equiv)	EtOH	reflux	60		
13	Et_3N (1 equiv)	H_2O	reflux	60		
14	L-proline (1 equiv)	MeOH	reflux	60	Trace	
15	pyridine (1 equiv)	MeOH	reflux	60	Trace	
16	piperidine (1 equiv)	MeOH	reflux	60	Trace	

the indolo[2,1-*b*]quinazoline systems leads to more significant biological activity.[15]

A few reports are available on the synthesis of γ-spirolactones, γ-spiroiminolactones,[16,17] and spiroquinazoline derivatives,[18,19] using tryptanthyrin as one of the starting materials and spiroindoloquinazoline using ammonium acetate and DABCO.[20,21] We are reporting herewith a facile and efficient one-pot synthesis of functionalized spiroindoloquinazoline compounds involving a three-component condensation reaction catalyzed by triethylamine using the substrates tryptanthrin, an active methylene compound, and a nucleophile carried out in MeOH using triethylamine as the base catalyst under reflux conditions (Scheme 1).

Quantum chemical calculations such as DFT are of great interest in studying the properties of organic molecules and predicting the properties of the molecule with reasonable computational accuracy.[22] This could also provide extensive help in comparing the data with experimental results. Based on the literature survey, the crystal structure and theoretical calculations of this compound **4c** have not been reported so far. Therefore, in this view of advantages, we have made an attempt to study the molecule properties like geometrical parameters, chemical reactivity, dipole moment, vibrational energies, molecular energies, and so forth. By the DFT method using the B3LYP/6-311G(d,p) basis set and using the optimized structure, we have calculated all the properties of the optimized molecule. Apart from this, we have also tried to find out the electronic properties of the molecule using the TD-DFT method.[22] Pharmacological significance of these compounds encourages us to perform the small molecule docking analysis of this class of compounds. It is a computational technique and helps in predicting the interactions between compounds and the protein receptors. We have performed the docking analysis of compound **4c** using Autodock vina.[23]

MATERIALS AND METHODS

Experimental Section. All the chemicals were used as received from Sigma-Aldrich (USA), Spectrochem (India), and SRL (India). Melting points were recorded in open capillaries and are uncorrected. Fourier transform infrared spectra (FT-IR) were recorded in the wave number range of 4000−400 cm^{-1} and are recorded on a Thermo Mattson Satellite FT-IR spectrophotometer. Nuclear magnetic resonance (NMR) spectra were recorded on a Bruker UltraShield spectrometer (400 and 100 MHz) or Bruker UltraShield spectrometer (300 and 75 MHz) in a DMSO-d_6 solvent using TMS as an internal

https://doi.org/10.1021/acsomega.1c06781
ACS Omega 2022, 7, 7874−7884

Table 2. Synthesis of Spiroindoloquinazoline Compounds

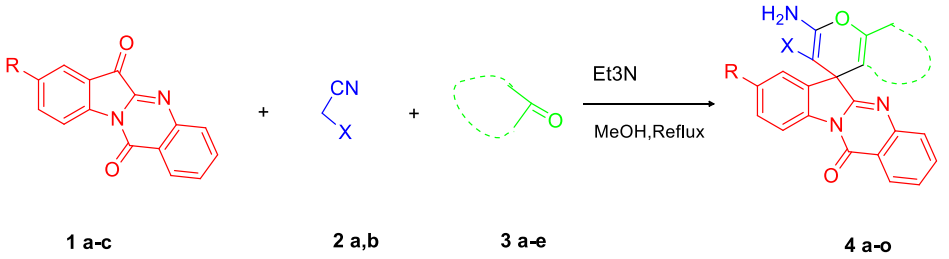

1 a-c 2 a,b 3 a-e 4 a-o

R = 1a = H, 1b = Br, 1c = NO_2 X= 2a = CN,2b = CO_2Et

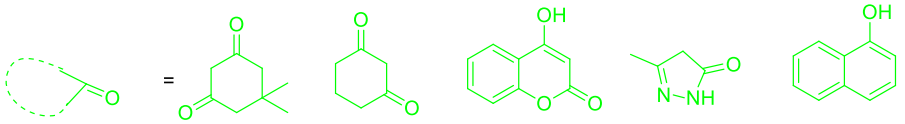

3 a-e 3a 3b 3c 3d 3e

entry	tryptanthrin 1	active methylene compound 2	nucleophile 3	time (min)	product/[yield %]	observed m. pt.	reported m. pt. (references)
1	**1a**	**2a**	**3a**	60	**4a** [85]	296−298	>270[20]
2	**1a**	**2a**	**3b**	60	**4b** [86]	266−268	>270[20]
3	**1a**	**2a**	**3d**	60	**4c** [86]	296−298	this work
4	**1a**	**2a**	**3e**	90	**4d** [88]	305−310	this work
5	**1a**	**2b**	**3a**	90	**4e** [82]	262−265	this work
6	**1a**	**2b**	**3b**	90	**4f** [84]	212−214	this work
7	**1a**	**2b**	**3c**	90	**4g** [88]	258−260	this work
8	**1a**	**2b**	**3d**	60	**4h** [82]	226−230	this work
9	**1b**	**2a**	**3a**	90	**4i** [86]	305−310	>270[20]
10	**1b**	**2a**	**3b**	90	**4j** [85]	264−268	>270[20]
11	**1b**	**2a**	**3c**	90	**4k** [81]	242−246	>270[20]
12	**1b**	**2a**	**3d**	90	**4l** [86]	212−214	this work
13	**1c**	**2a**	**3a**	120	**4m** [87]	278−280	this work
14	**1c**	**2a**	**3b**	90	**4n** [88]	254−256	this work
15	**1c**	**2a**	**3d**	120	**4o** [85]	212−214	this work

standard. Mass spectra were recorded on a Water-s(R)Micromass(R)Q-TOF Micro mass spectrometer. Solvents used were of commercial grade and purified before use by distillation.

General Procedure for the Synthesis of Compound 4. A mixture of tryptanthrins (**1a**−**c**) (1 mmol), malononitrile or ethylcyanoacetates (**2a**,**b**) (1 mmol), and nucleophiles (**3a**−**e**) (1 mmol) and triethylamine (1.2 mmol) in MeOH (5 mL) was stirred under reflux conditions for the time indicated in Table 2. After completion of the reaction, the solvent was evaporated under a vacuum. The residue was extracted with ethyl acetate, washed with 10% HCl, and then neutralized with 5% Na_2CO_3 and dried over anhydrous Na_2SO_4. The solvent was removed to dryness which was purified by flash column chromatography (silica gel, mixtures of petroleum ether/ethyl acetate) to afford desired pure products **4**.

RESULTS AND DISCUSSION

As the first step, the reaction between tryptanthrin **1a**, malononitrile **2a**, and dimedone **3a**, as a model reaction, was investigated under solvent- and catalyst-free conditions. Only dicyanomethylene adduct **5a** was obtained in 92% yield, and expected product **4a** was not observed (Table 1, entry 1). Even when the reaction was carried out in MeOH under catalyst-free conditions, only dicyanomethylene derivative **5a** was obtained in 93% yield (Table 1, entry 2). When the above-mentioned reaction was carried out with various catalysts such as montmorillonite-K10 clay, I_2, and Amberlite IRA-400 Cl in MeOH under reflux conditions too, only **5a** was obtained (Table 1, entries 3−5). When the reaction of tryptanthrin **1a**, malononitrile **2a**, and dimedone **3a** in MeOH and the presence of the Et_3N catalyst under reflux conditions was carried out, **4a** was obtained as the major product and **5a** as a minor product (Table 1, entry 6). When this reaction was also carried out at room temperature, the yield of **4a** was decreased and that of **5a** was increased (Table 1, entry 7). When the catalyst load was doubled, there was no significant change in yield, and a lower catalyst load led to a lower yield of **4a** (Table 1, entry 8, 9). The reaction was also carried out in various solvents such as DMSO, MeCN, EtOH, and H_2O. Product yields in DMSO were similar to those in MeOH, and the remaining solvents were found to be not suitable (Table 1, entry 10−13). Other amines such as L-proline, pyridine, and piperidine failed to catalyze the reaction (Table 1, entry 14−16). Therefore, the optimum conditions for this reaction are refluxing in solvents such as MeOH and DMSO and using Et_3N as a catalyst.

The condensation reaction of an equal ratio of tryptanthrin (**1a**), malononitrile (**2a**), and dimedone (**3a**) in the presence

https://doi.org/10.1021/acsomega.1c06781
ACS Omega 2022, 7, 7874−7884

Scheme 2. Plausible Mechanism for the Formation of Compound 4

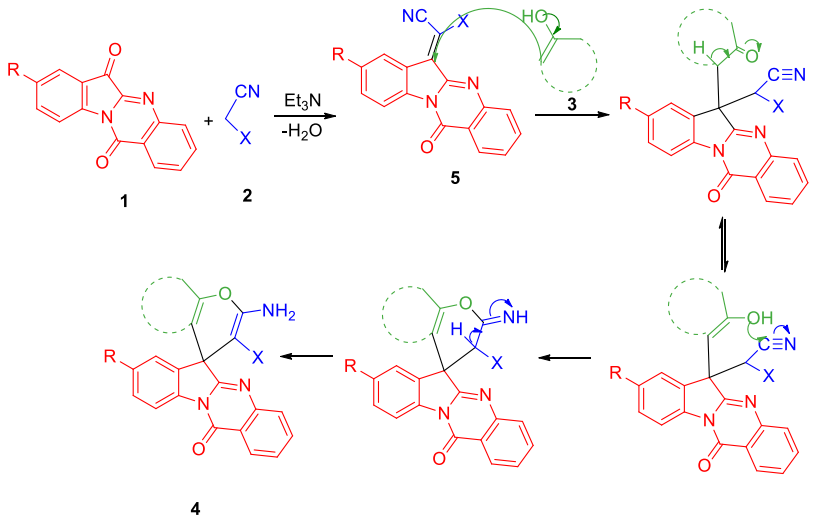

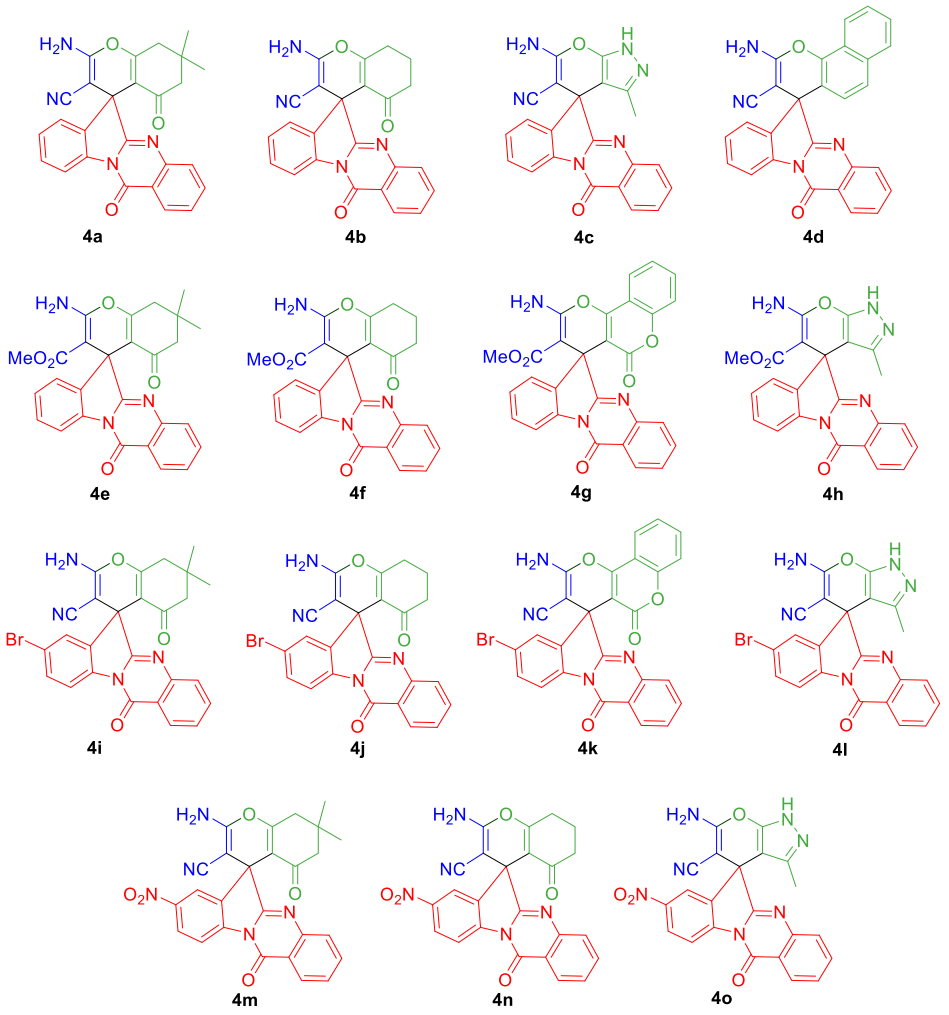

Figure 1. Spiroindoloquinazoline compounds from **4a−o**.

of 1 equiv of triethylamine in MeOH under reflux conditions furnished 2-amino-7,7-dimethyl-5,12′-dioxo-5,6,7,8-tetrahydro-12′*H* spiro[chromene-4,6′-indolo(2,1-*b*)quinazoline]-3-carbonitrile **4a** with 84% yield within 60 min. Encouraged by this result, we extended the reaction of tryptanthrins (**1a−c**) and cyanoacetic acid derivatives **2a,b** (cyanoacetic ester, malononitrile) with other nucleophiles **3a−e** (1,3-dicarbonyl compounds, 3-methyl-1*H*-pyrazol-5-one, and 1-naphthol) under similar conditions (MeOH/triethylamine) which gave corresponding compounds of spiroindoloquinazoline compounds, **4a−o**, in moderate to high yields (84−87%), and the results are summarized in Table 2. However, when the reaction

https://doi.org/10.1021/acsomega.1c06781
ACS Omega 2022, 7, 7874−7884

was carried out with ethyl cyanoacetate **2b** at room temperature, it showed a combination of starting materials, and product **4** was obtained only in trace amounts. When the reaction was carried out in EtOH under reflux conditions, only the starting compounds (**3a**−**e**) were obtained with trace amounts of product **4**. Interestingly, we found that MeOH under reflux conditions proceeded and gave unexpected products **4e**−**h** (Table 2), and it was observed that compound **4e** by the ^{1}HNMR spectrum showed a single peak at δ 3.15 ppm confirming the presence of the methoxy group. The ^{13}C NMR spectrum also demonstrates that the resonance peak at 49.8 corresponds to the methoxy group. Moreover, the presence of the molecular ion peak at 470.1724 $(M)^{+}$ in the mass spectrum was due to the formation of compound **4e**. All these results suggest that the ethyl group of the ester is replaced by the methyl group originating from the solvent, MeOH.

It was observed that electron-withdrawing groups such as bromo and nitro substituted on tryptanthrins did not alter the yield of the products. Among the various nucleophiles, dimedone **3a**, 1,3-cyclohexanedione **3b**, 4-hydroxycoumarin **3c**, 3-methyl-1*H*-pyrazol-5-one **3d**, and 1-naphthol **3e** gave the best yield. Good yield was also observed for 1,3-cyclohexanedione **3b** and dimedone **3a** (86, 85%, respectively) as a nucleophile. Significantly, the reaction with 3-methyl-1*H*-pyrazol-5-one **3d** also afforded a good yield (Table 2, entry 3). When the reaction was carried out with 3-methyl-1*H*-pyrazol-5-one **3d**, trypthanthrins (**1a**−**c**), and active methylene compounds (**2a**,**b**) in MeOH, better yields (82—86%) were observed under reflux conditions compared to the same reaction carried out at room temperature (40%).

The reaction between tryptanthrin **1a**, malononitrile **2a**, and dimedone **3a** was carried out to produce 2-amino-7,7-dimethyl-5,12′-dioxo-5,6,7,8-tetrahydro-12′*H* spiro[chromene-4,6′-indolo(2,1-*b*)quinazoline]-3-carbonitrile **4a** (shown in Scheme 2). In the first step of the reaction, possibly the Knoevenagel reaction between tryptanthrin **1a** and malononitrile **2a** leads to the formation of dicyanomethylene derivative **5a**. The subsequent hydroxide-promoted Michael addition of cyclic 1,3-diketone **3a** to **5a** results in electron-deficient 2-amino-7,7-dimethyl-5,12′-dioxo-5,6,7,8-tetrahydro-12′*H* spiro-[chromene-4,6′-indolo(2,1-*b*)quinazoline]-3-carbonitrile **4a**.

All the synthesized compounds were characterized and confirmed using spectroscopic techniques (IR, ^{1}HNMR, ^{13}CNMR, and HRMS). Final structure proof of compound **4c** was obtained from single-crystal X-ray studies (Figure 1).[25]

COMPUTATIONAL DETAILS

Computational studies of synthesized compound **4c** was carried out in the DFT method using Gaussian 09 software[24] and the B3LYP/6-311 G(d,p) basis set, and the optimized molecular structure was predicted. The geometrical parameters like bond length and bond angle of the compound were analyzed using Chemcraft software. Theoretical vibrational frequency data are compared with experimental results, and they are in good agreement with each other. The TD-DFT method was employed to study the electronic properties of the compound in DMSO as the solvent. Also, the frontier molecular orbital energies (FMO) were calculated as the energy gap between HOMO and LUMO helps us to predict the reactivity of the compound. The molecular electrostatic potential (MEP) is viewed using GaussView software. To learn about the nonlinear optical properties of the molecule, dipole moment and polarizability were theoretically calculated. The molecular docking studies were carried out using Autodock vina software.

Molecular Geometry. Single-crystal XRD of compound **4c** was done using a crystal of dimension 0.35 × 0.30 × 0.25 mm^3 with graphite monochromatic Mo Kα radiation (0.71073). The studied compound has a space group of $P2_1/c$, and the unit cell parameters are a = 11.3245(4) Å, b = 12.1767(5) Å, C = 17.3982(8) Å, α, γ = 90°, β = 104.506°,V = 2322.64(17) Å^3, and Z = 4. The crystallographic details are given in Table 3.

Table 3. Crystallographic Data of Compound 4c

identification code	945,362
empirical formula	$C_{24}H_{20}N_6O_3S$
formula weight	472.52
temperature/K	293(2)
space group	$P2_1/c$
a/Å	11.3245(4)
b/Å	12.1767(5)
c/Å	17.3982(8)
α/°	90.00
β/°	104.506(2)
γ/°	90.00
volume/Å^3	2322.64(17)
Z	4
ρ_{calc}g/cm^3	1.351
μ/mm^{-1}	0.178
F(000)	984.0
crystal size/mm^3	0.35 × 0.30 × 0.25
Radiation	Mo Kα (λ = 0.71073)
2Θ range for data collection/°	3.72 to 55
index ranges	$-9 \le h \le 14$, $-13 \le k \le 15$, $-22 \le l \le 22$
reflections collected	24,269
independent reflections	5337 [Rint = 0.0344, R_{sigma} =]
data/restraints/parameters	5337/7/337
goodness-of-fit on F^2	1.027
final R indexes [$I \ge 2\sigma$ (I)]	$R1$ = 0.0579, wR_2 = 0.1537
final R indexes [all data]	$R1$ = 0.0862, wR_2 = 0.1751
largest diff. peak/hole/e Å^{-3}	0.77/−0.68

The crystallographic structure obtained by solving the structure using SHELX was used to optimize the structure, and the ORTEP diagram of the compound is given in Figure 2.[25]

From the optimized structure, the geometrical parameters (bond length and bond angle) were calculated theoretically. The calculated parameters are given in Table S1. A plot of the calculated and experimental bond length and bond angle is done to check the accuracy of calculation and is shown in Figure 3.

From the graph, a linear relationship was observed between experimental and theoretical values of the bond length and bond angle. The correlation coefficient (R^2) calculated was unity and 0.9938 for the bond length and bond angle, respectively, which shows good agreement between experimental and theoretical results.

Furthermore, the compound is analyzed with weak hydrogen bonding between N−H···O, and this plays an important role in the stability of the molecule.

https://doi.org/10.1021/acsomega.1c06781
ACS Omega 2022, 7, 7874−7884

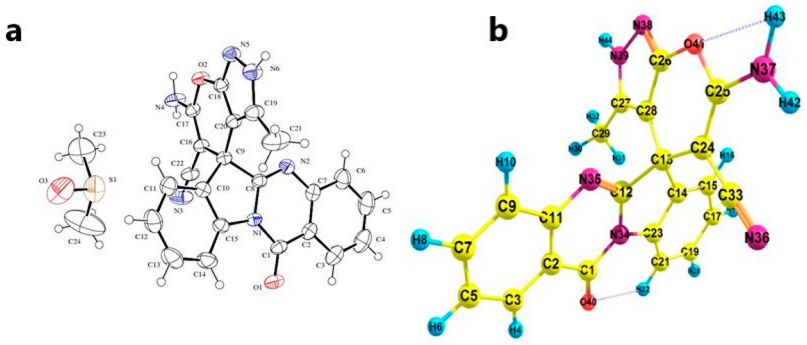

Figure 2. (a) ORTEP diagram and (b) optimized structure.

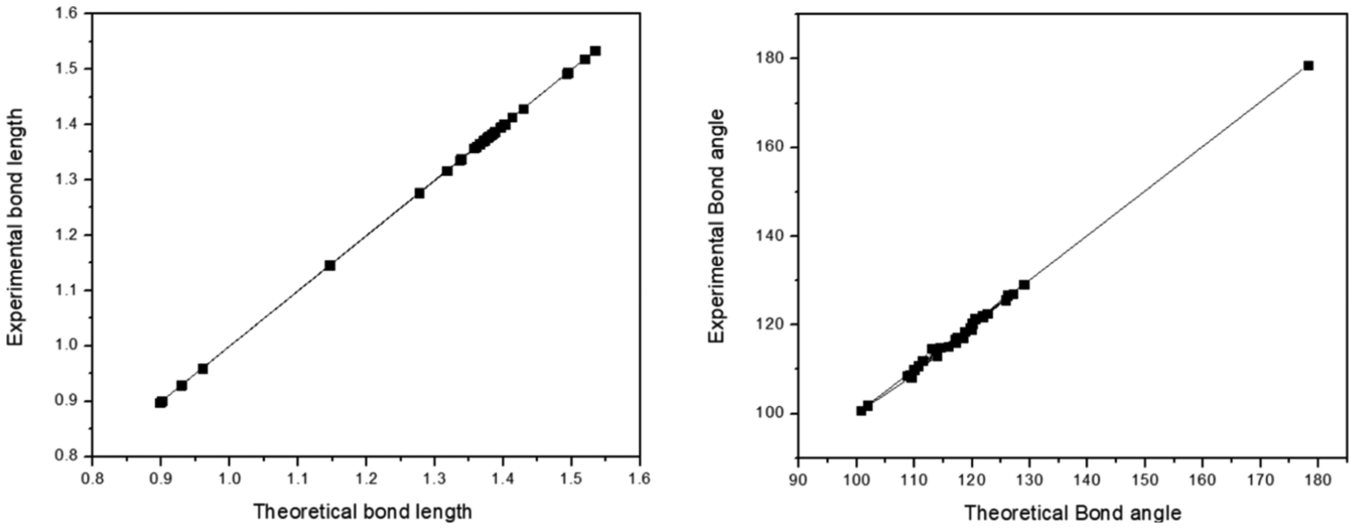

Figure 3. Plot of calculated versus experimental bond lengths and bond angles.

Frontier Molecular Orbital Analysis. FMO analysis explains the chemical reactivity of a compound which includes two molecular orbitals such as HOMO or highest occupied molecular orbital and LUMO or lowest unoccupied molecular orbital. HOMO is the outermost orbital with electrons, and it acts as a donor, whereas LUMO is the outermost orbital without electrons, and it acts as an acceptor. The HOMO−LUMO plot is given in Figure 4. The HOMO energy is calculated as −6.0208 eV, and LUMO energy is −1.3285, and the energy gap which is the difference in energies of HOMO and LUMO predicts that the reactivity of the molecule is 4.6924 eV.

In addition to this, it also helps us to calculate various other factors like chemical hardness (η), electron affinity (EA), ionization potential (IP), electrophilicity (ω), and electronegativity (χ) using the equations derived from the Koopmans theorem[26] and are given in Tables 4 and 5.

$$\text{ionization potential (IP)} = -E_{\text{HOMO}} \quad (1)$$

$$\text{electron affinity (EA)} = -E_{\text{LUMO}} \quad (2)$$

$$\text{the hardness } (\eta) = \frac{\text{IP} - \text{EA}}{2} \quad (3)$$

$$\text{the softness (S)} = \frac{1}{2\eta} \quad (4)$$

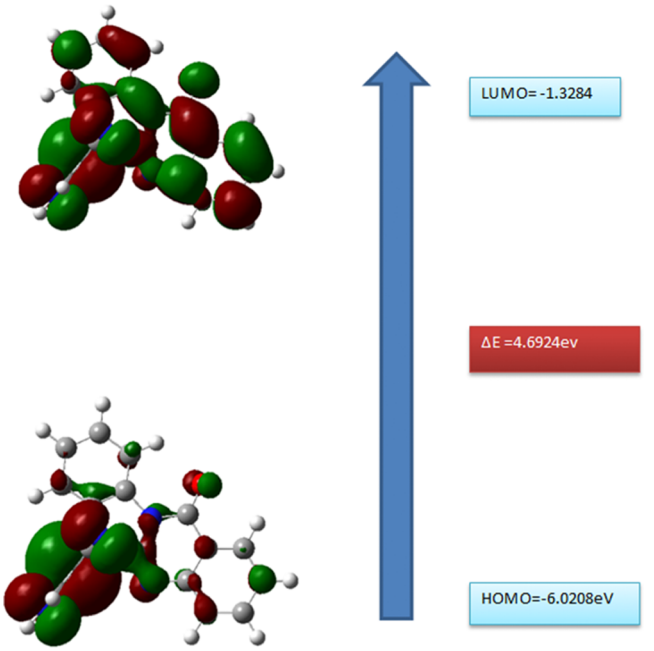

Figure 4. Frontier molecular orbital of compound **4c**.

$$\text{the electronegativity } (\chi) = \frac{\text{IP} + \text{EA}}{2} \quad (5)$$

https://doi.org/10.1021/acsomega.1c06781
ACS Omega 2022, 7, 7874−7884

Table 4. Hydrogen Bond Measurements for Compound 4c

D	H	A	d(D−H)/Å	d(H−A)/Å	d(D−A)/Å	D−H−A/°
N4	H4A	O1[1]	0.900(10)	2.028(12)	2.898(3)	162(2)
N4	H4B	N5[2]	0.897(10)	2.073(10)	2.968(3)	176(2)
N6	H6A	O3[3]	0.900(10)	1.893(11)	2.790(5)	174(3)

$$\text{Global electrophilicity index } (\omega) = \frac{\mu^2}{2\eta} \quad (6)$$

Table 5. Global Reactivity Parameters of Compound 4c

orbital energy	energy (eV)
E_{HOMO}	−6.02084
E_{LUMO}	−1.3285
ΔE	4.6924
chemical potential (μ)	−6.6857
chemical hardness (η)	2.34615
softness (S)	0.2131
electronegativity(χ)	6.6857
Global electrophilicity index (ω)	9.5259

Molecular Electrostatic Potential. The MEP is a three-dimensional plot that helps to predict the interaction of the molecule with its surrounding molecules.[27] The MEP predicts the site of electrophilic and nucleophilic attack. The different color regions in the MEP plot represent different electrostatic potentials. The red region represents the most negative electrostatic potential, and blue represents the most positive electrostatic potential, and green represents zero electrostatic potential. The MEP plot of compound **4c** is given in Figure 5.

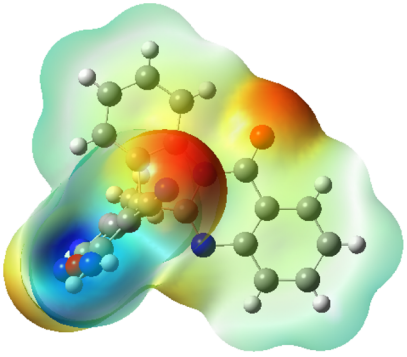

Figure 5. Molecular electrostatic potential diagram of compound **4c**.

The color code of this electron density diagram lies in the range of −8.234 and 8.234 a.u. The negative region is around oxygen and nitrogen atoms. The red color around the O atom indicates the possibility of hydrogen bonding. The positive region is around the N atom.

Electronic Properties. The electronic spectrum of the molecule provides a deep insight into the charge transfer in the excited and ground state of the molecule. Thus, to record UV visible absorption spectra of the compound, the TD-DFT method was employed using the B3LYP basis set and Gaussian 09 package. The absorption spectra of compound **4c** are obtained as shown in Figure 6.

In an organic molecule, absorption spectra may be observed due to transitions from $\pi-\pi^*$ and/or $n-\pi^*$ in the range of 200−700 nm. In compound **4c**, the maximum absorption peak

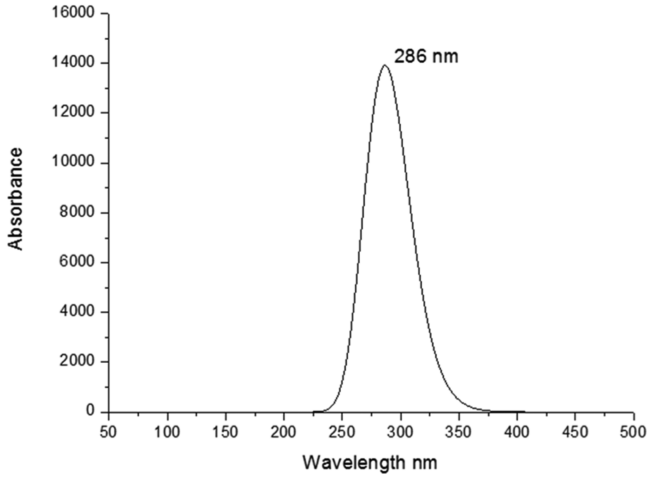

Figure 6. Absorption spectra of compound **4c**.

(λ_{max}) is observed at 284.67 nm with an oscillator strength of 0.2816.

Non-linear Optical Studies. Organic NLO properties have been at the forefront in the recent past, as they have gained their importance in telecommunications, signal processing, and optical interconnections.[28] Therefore, we computed the total dipole moment (μ), polarizability (α), and first-order hyper polarizability (β) of compound **4c** as shown in Table 6.

$$\text{total static dipole moment } \mu = \sqrt{\mu_x^2 + \mu_y^2 + \mu_z^2} \quad (7)$$

$$\text{the mean polarizability } \alpha = \frac{\alpha_{xx} + \alpha_{yy} + \alpha_{zz}}{3} \quad (8)$$

the anisotropy of polarizability

$$\Delta\alpha = \frac{1}{\sqrt{2}}\sqrt{(\alpha_{xx} - \alpha_{yy})^2 + (\alpha_{yy} - \alpha_{zz})^2 + (\alpha_{zz} - \alpha_{xx})^2 + 6\alpha_{xx}^2} \quad (9)$$

The complete equation for calculating the magnitude of the first-order hyper polarizability is as follows

$$\beta = \sqrt{(\beta_{xxx} + \beta_{xyy} + \beta_{xzz})^2 + (\beta_{yyy} + \beta_{xxy} + \beta_{yzz})^2 + (\beta_{zzz} + \beta_{xxz} + \beta_{yyz})^2} \quad (10)$$

From the calculations, it is observed that the dipole moment of the compound is 4.8418 Debye units, and the polarizability (α_{total}) is 4.05×10^{-23}, and the first-order polarizability is 1.0266×10^{-30}. NLO properties of compound **4c** are greater than those of urea which is considered to be the prototypical compound. Theoretically, the NLO property of the compound is greater than that of urea, which makes it a good NLO component.

Vibrational Analysis. The theoretical FT-IR spectrum of the compound was deduced by using the B3LYP/6-311G (d,p) basis set and compared with the experimental FT-IR data. Both the theoretical and experimental responses are illustrated in Figures 7 and 8.

https://doi.org/10.1021/acsomega.1c06781
ACS Omega 2022, 7, 7874−7884

Table 6. Polarizability Characteristics of Compound 4c

components of μ	values	components of α	values	components of β	Values
μ_x	−1.8586	α_{xx}	−157.766	β_{xxx}	53.9989
μ_y	−1.5608	α_{yy}	−165.2621	β_{yyy}	12.727
μ_z	−4.1896	α_{zz}	−163.978	β_{zzz}	−125.4794
μ(D)	4.841822	α_{xy}	−13.4191	β_{xyy}	−17.2272
		α_{xz}	−4.2283	β_{xxy}	−47.194
		α_{yz}	−12.6253	β_{xxz}	30.3625
		α (a.u)	−162.3353667	β_{xzz}	−66.7209
		α (e.s.u)	−2.40581E−23	β_{yzz}	−61.1666
		$\Delta\alpha$ (a.u)	273.3469351	β_{yyz}	31.2512
		$\Delta\alpha$ (e.s.u)	4.051×10^{-23}	β_{xyz}	38.4196
				βtot (a.u)	118.8342
				βtot e.s.u	1.026×10^{-30}

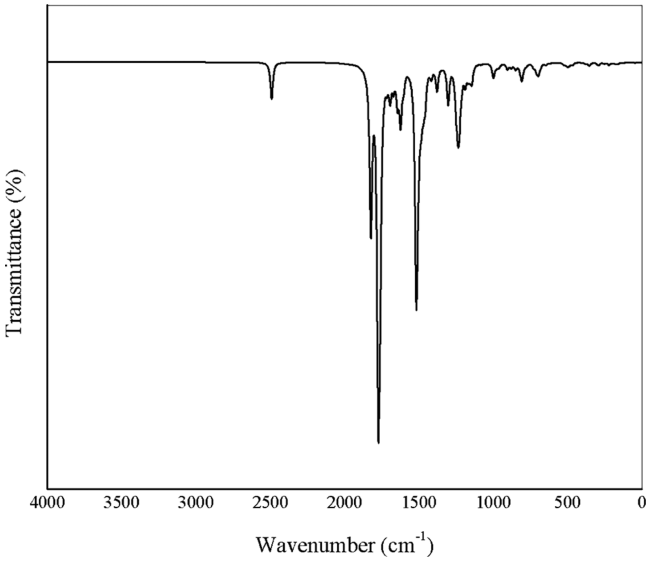

Figure 7. Theoretical FT-IR spectrum.

There is a slight difference in the position of peaks. The −CN peak is observed at 2190 cm^{-1} in experimental observation. However, when calculated theoretically, there is a slight difference, and it appears at 2500 cm^{-1}. The slight deviations in theoretical intensities from the experimental values may be attributed to the fact that the theoretical wave numbers are obtained from the isolated molecule in the gaseous phase, and the experimental wave numbers are obtained from the isolated molecule in the solid state.

Molecular Docking. Molecular docking is an important technique in drug discovery. Molecular docking provides computer-assisted drug design. It is a convenient tool that helps to study the mechanism of protein−ligand interactions and helps in analyzing the protein ligand-binding site.

The phospholipase inhibitory effect of these molecules are already explored using molecular docking studies.[20] Thus, we decided to carry out the molecular docking studies of compound **4c**, to check other significant biological activity of the compound. The smile format of the compound was used in PASS online (prediction of activity of spectra for substances). This provides an insight into the various biological activities of the compound, like Hepatic disorder treatment, liver fibrosis treatment, antiallergic, antimitotic, and antiasthmatic treat-

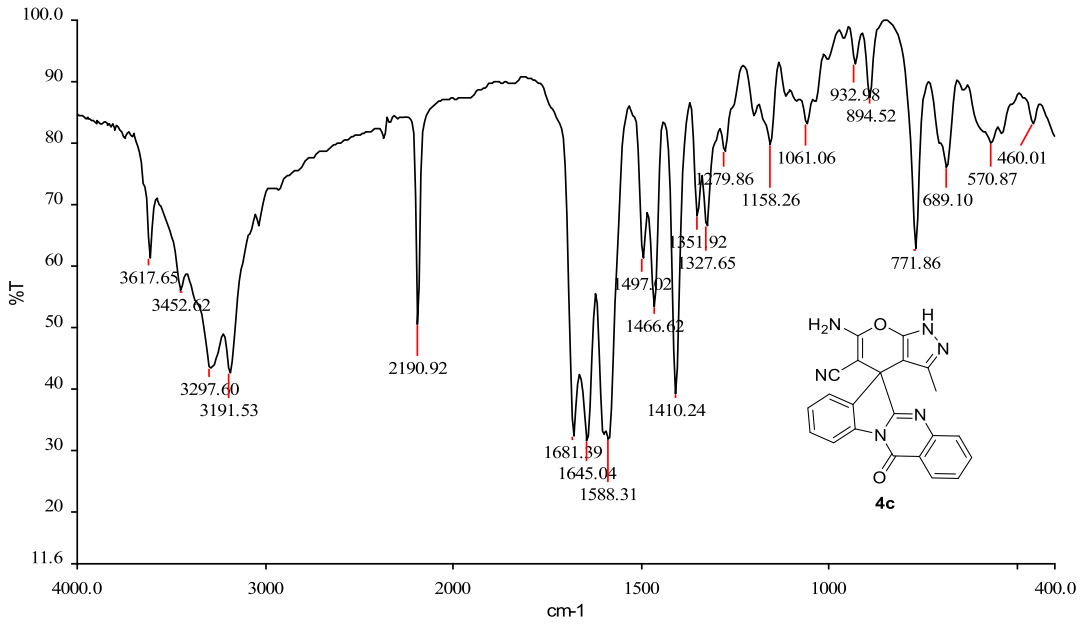

Figure 8. Experimental FT-IR spectrum **4c**.

https://doi.org/10.1021/acsomega.1c06781
ACS Omega 2022, 7, 7874−7884

ments. It can also act as a fibroblast growth factor agonist with a high P_a (probability to be active) value of 0.671. Two proteins were chosen out of the various choices according to their characteristics that meet docking conditions. Two target proteins 4POK and 4IZE of resolution 1.70 and 2.00 A^0, respectively, were chosen for docking.

Both ligand and target proteins were prepared for docking analysis in Pymol software. Dock suite 4.2.6 software was used for studying the interaction between the protein and ligand and their binding affinity. The Lamarckian Genetic Algorithm (LGA) feature in Auto Dock software was utilized for the docking process. Discovery Studio Visualizer 4.0 software was used to visualize the interaction of the ligand with the target protein. The molecular interaction between the ligand and protein along with their binding site is illustrated in Figure 9.

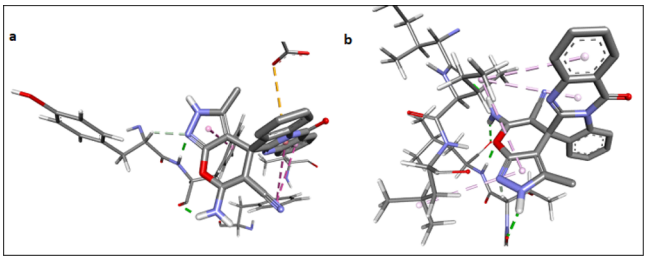

Figure 9. Diagrammatic representation of ligand interactions with proteins (a) 4POK and (b) 4IZE.

The various parameters of docking are listed in Table 7. Table 7 gives information about the target protein bond

Table 7. Docking Parameters of Ligand (Compound) 4c

protein (PDB)	bond distance (Å)	estimated inhibition constant (μM)	binding energy (kcal/mol)	intermolecular energy (kcal/mol)	RMSD
4POK	5.75, 5.32, 5.04, 4.91, 4.58, 2.62, 1.94, 1.98	8.64	- 6.91	−7.21	29.48
4IZE	5.36, 5.03, 4.82, 4.78, 2.20, 2.14, 1.93, 1.91, 1.86	2.19	- 7.72	−8.02	20.01

distance, inhibition constant, and RMSD values. The inhibition constant (ki) value provides information regarding the medication required to inhibit the activity of the protein. The obtained inhibition constant for the ligand with two given target proteins 4POK and 4IZE is 29.05 and 19.02 μM, respectively. The binding energy exhibited by these proteins 4POK and 4IZE is −6.91 and −7.72 kcal/mol, respectively. Lower binding energy is shown by the 4IZE protein which suggests that this protein can bind easily with a ligand molecule. Also, a lower inhibition constant for the protein 4IZE suggests that only less quantity of medication is required in the case of this protein.

The binding of various enzymes on the ligand and the type of bond formed by them are shown in Figure 10; the PHE A:151 forms hydrogen bonding with the nitrogen atom of $-NH_2$ and the pyrazole ring of the ligand. The amino acid TYR A 150 forms a carbon−hydrogen bond with the ligand, and the amino acid VAL A44 forms a π-alkyl bond with the benzene ring. PHE A:9 forms a $\pi-\pi$ stacked and $\pi-\pi$ T-shaped bond with the benzene ring.

Figure 10 explains that the amino acid ILE A:149, LEU A:97, and PRO A:95 forms hydrogen bonding with the ligand molecule, whereas amino acids ILE A:150 and lEU A:151 form a π-alkyl bond with the ligand. These computational explanations suggest that this compound can act against 4POK and 4IZE as fibroblast growth factor agonists.

CONCLUSION

In summary, we have developed an easy and clean one-pot, three-component reaction for the synthesis of spiroindoloquinazoline compounds in methanol in the presence of triethylamine as a catalyst. This method is simple, efficient, and comes with easy work-up procedures. Theoretical DFT calculations were performed for compound **4c,** and the properties were in good agreement with the experimental values. Molecular docking was also carried out for selective compound **4c** as the ligand and using two proteins 4POK and 4IZE, and the results suggest that the ligand binds actively with the target protein and indicate that compound **4c** can act as a fibroblast growth factor agonist.

Spectroscopic Data for Selected Compounds. (**4a**): White solid, mp 296 °C; Rf (40% EtOAc−petroleum ether) 0.69, FT-IR ν_{max} (KBr): 3408, 3276, 2198, 1660, 1600, 1464, 1358, 1322, 1266 cm^{-1}; ^{1}H NMR (300 MHz, DMSO-d_6): δ = 8.45 (d, 1H, J = 8.1 Hz, ArH), 8.33 (d, 1H, J = 7.8 Hz, ArH), 7.88−7.76 (m, 2H, ArH), 7.66−7.63 (m, 1H, ArH), 7.55 (s, 2H, NH_2), 7.52−7.35 (m, 3H, ArH), 2.70−2.67 (m, 2H, CH_2), 2.11−2.10 (m, 2H, CH_2), 1.05 (s, 3H, CH_3), 1.01 (s, 3H, CH_3); ^{13}C NMR (75 MHz, DMSO-d_6): δ = 195.4, 164.4, 162.6, 158.9, 158.3, 147.1, 138.6, 135.6, 134.9, 129.1, 127.3, 127.1, 126.4, 123.8, 120.6, 117.3, 115.8, 111.2, 57.9, 49.8, 47.8, 40.3, 32.1, 27.4, 27.0; HRMS m/z calcd for $C_{26}H_{21}N_4O_3$, $(M + H)^+$ 437.1623; found, 437.1614.

(**4e**): White solid, mp 262 °C; Rf (40% EtOAc−petroleum ether) 0.66, FT-IR ν_{max} (KBr): 3346, 3077, 2954, 1684, 1603, 1463, 1353, 1313, 1224 cm^{-1}; ^{1}H NMR (500 MHz, DMSO-d_6): δ = 8.62 (d, 1H, J = 7.5 Hz, ArH), 8.47 (d, 1H, J = 7.0 Hz, ArH), 7.72−7.71 (m, 2H, ArH), 7.51−6.79 (m, 6H, ArH, NH_2), 3.15 (s, 3H, OCH_3), 2.67−2.47 (m, 2H, CH_2), 2.18−2.03 (m, 2H, CH_2), 1.11 (s, 3H, CH_3), 1.03 (s, 3H, CH_3); ^{13}C NMR (125 MHz, DMSO-d_6): δ = 195.4, 164.9, 162.6, 158.9, 158.3, 147.1, 138.6, 135.6, 134.9, 129.1, 127.3, 127.1, 126.4, 123.8, 120.6, 117.2, 115.8, 111.2, 57.9, 49.8, 47.8, 40.3, 32.1, 27.4, 27.0; HRMS m/z calcd for $C_{27}H_{24}N_3O_5$, $(M + H)^+$ 470.1724; found, 470.1716.

(**4i**): White solid, mp 305 °C; Rf (40% EtOAc−petroleum ether) 0.67, FT-IR ν_{max} (KBr): 3406, 3270, 2960, 2196, 1659, 1598, 1465, 1354, 1320, 1221, 560 cm^{-1}; 7.49−6.47 (m, 8H, ArH, NH_2), 6.70 (s, 1H, ArH), 2.63 (s, 2H, CH_2), 2.22−2.17 (m, 2H, CH_2), 1.02−1.08 (s, 6H, CH_3); ^{13}CNMR (100 MHz, DMSO-d_6): δ = 195.9, 164.9, 163.2, 159.4, 158.8, 147.6, 139.0, 136.1, 135.4, 129.6, 127.9, 127.8, 127.6, 126.9, 124.3, 121.1, 117.8, 116.3, 111.7, 58.4, 50.3, 48.4, 32.6, 27.9, 27.5; HRMS m/z calcd for $C_{26}H_{19}N_4O_3BrNa$, $(M + Na)^+$ 537.0545; found, 537.0538.

(**4m**): White solid, mp 278 °C; Rf (40% EtOAc−petroleum ether) 0.71, FT-IR (KBr): ν_{max} = 3425, 2200, 1692, 1596, 1516, 1465, 1342, 1267, 1204; ^{1}HNMR (500 MHz, DMSO-d_6& $CDCl_3$): δ = 8.46 (d, J = 10.0 Hz, 1H, ArH), 8.32−8.18 (m, 1H, ArH), 7.82 (t, J = 9.5 Hz, 1H, ArH), 7.00−7.56 (m, 1H, ArH), 7.47−7.34 (m, 3H, NH_2, ArH), 7.14−7.11 (m, 1H,

https://doi.org/10.1021/acsomega.1c06781
ACS Omega 2022, 7, 7874−7884

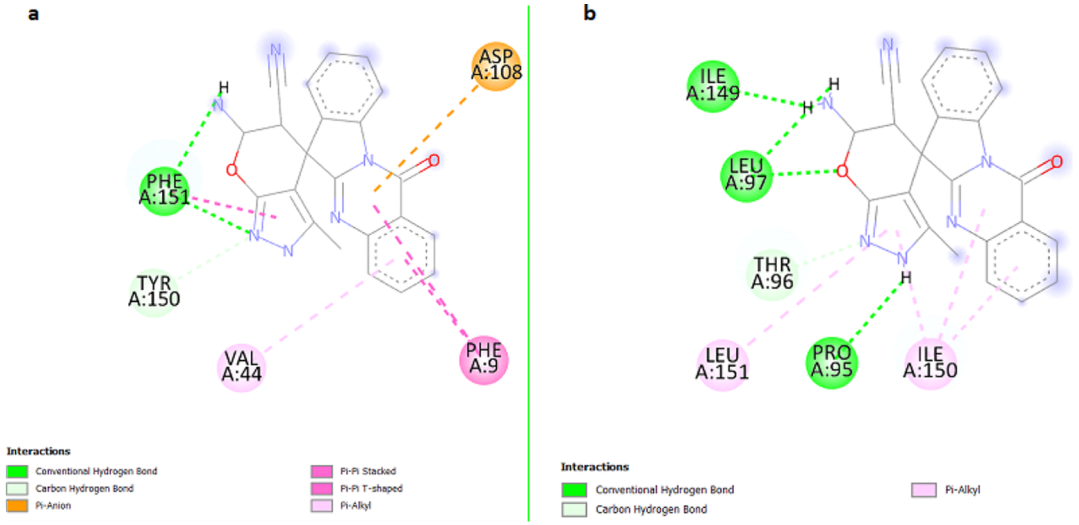

Figure 10. Binding activity of various enzymes of proteins on the ligand: (a) 4POK and (b) 4IZE.

ArH), 2.71−2.59 (m, 2H, CH_2), 2.14−2.04 (m, 2H, CH_2), 1.05 (s, 3H, CH_3), 1.02 (s, 3H, CH_3); ^{13}C NMR (125 MHz, DMSO-d_6): δ = 195.2, 164.5, 159.4, 159.2, 147.6, 139.1, 134.8, 129.4, 128.5, 127.6, 127.5, 126.8, 123.9, 123.3, 122.1, 121.2, 117.7, 116.3, 109.8, 78.9, 57.9, 50.4, 47.3, 39.3, 32.3, 27.7, 27.6; ESI m/z calcd for $C_{26}H_{19}N_5O_5$, 481.4596; found, 481.4595.

DATA AND SOFTWARE AVAILABILITY

In our study, computational studies were carried out using the Gaussian 09 package which is available at www.gaussian.com.PDB structures are available from RCSBPDB (https://www.rcsb.org). Molecular docking studies were performed using software AutoDock Tools. (http://autodock.scripps.edu/resources/adt).The ligand and protein molecule preparation was done using PYMOL which is available at http://pymol.sourceforge.net.The docked structures were viewed in Discovery Studio which can be obtained from https://discover.3ds.com/discovery-studio-visualizer.The FT-IR spectra were drawn using Origin Lab which is available at https://www.originlab.com. Produced and analyzed data are available from the authors upon request.

ASSOCIATED CONTENT

Supporting Information

The Supporting Information is available free of charge at https://pubs.acs.org/doi/10.1021/acsomega.1c06781.

Experimental procedures and compound characterization data (PDF)

AUTHOR INFORMATION

Corresponding Author

Harichandran Gurusamy − *Department of Polymer Science, University of Madras, Chennai 600 025, India;* orcid.org/0000-0003-3106-0578; Phone: +919444628300; Email: umghari@gmail.com, umhari@unom.ac.in

Authors

Surya Cholayil Palapetta − *Department of Polymer Science, University of Madras, Chennai 600 025, India*

Sarojinidevi Krishnan − *Department of Polymer Science, University of Madras, Chennai 600 025, India*

Shanmugam Ponnusamy − *Organic Chemistry Division, CSIR-Central Leather Research Institute, Chennai 600 020, India;* orcid.org/0000-0003-0411-1982

Complete contact information is available at: https://pubs.acs.org/10.1021/acsomega.1c06781

Notes

The authors declare no competing financial interest.

ACKNOWLEDGMENTS

Authors thank the University of Madras for providing infrastructure facilities, Director, CSIR-CLRI, for providing NMR measurement, and SAIF-IITM for single-crystal measurement. SCP thanks RUSA for providing the project fellowship under RUSA 2.0 (C3/RI&QI/T2/P3/PF1).

REFERENCES

(1) (a) Zhu, J.; Bienaymé, H. *Multicomponent Reactions*; Wiley-VCH: New York, 2005. (b) Dondoni, A.; Massi, A. Design and Synthesis of New Classes of Heterocyclic C-Glycoconjugates and Carbon-Linked Sugar and Heterocyclic Amino Acids by Asymmetric Multicomponent Reactions (AMCRs). *Acc. Chem. Res.* **2006**, *39*, 451−463.

(2) Ramón, D. J.; Yus, M. Asymmetric Multicomponent Reactions (AMCRs).The New Frontier. *Angew. Chem., Int. Ed.* **2005**, *44*, 1602−1634.

(3) Sarges, R.; Howard, H. R.; Browne, R. G.; Lebel, L. A.; Seymour, P. A.; Koe, B. K. 4-Amino[1,2,4]triazolo[4,3-a]quinoxalines.A novel class of potent adenosine receptor antagonists and potential rapid-onset antidepressants. *J. Med. Chem.* **1990**, *33*, 2240−2254.

(4) Badran, M. M.; Moneer, A. A.; Refaat, H. M.; El-Malah, A. A. Synthesis and antimicrobial activity of novel quinoxaline derivatives. *J. Chin. Chem. Soc.* **2007**, *54*, 469−478.

(5) Hazeldine, S. T.; Polin, L.; Kushner, J.; White, K.; Bouregeois, N. M.; Crantz, B.; Palomino, E.; Corbett, T. H.; Horwitz, J. P. II. Synthesis and Biological Evaluation of Some Bioisosteres and Congeners of the Antitumor Agent, 2-{4-[(7-Chloro-2-quinoxalinyl)-oxy] phenoxy}propionic acid (XK469). *J. Med. Chem.* **2002**, *45*, 3130−3137.

(6) Bonsignore, L.; Loy, G.; Secci, D.; Calignano, A. Synthesis and pharmacological activity of 2-oxo-(2H) 1-benzopyran-3-carboxamide derivatives. *Eur. J. Med. Chem.* **1993**, *28*, 517−520.

(7) Recio, M.-C.; Cerdá-Nicolás, M.; Potterat, O.; Hamburger, M.; Ríos, J.-L. Anti-inflammatory and antiallergic activity in vivo of

lipophilic Isatis tinctoria extracts and tryptanthrin. *Planta Med.* **2006**, *72*, 539−546.
(8) Takei, Y.; Kunikata, T.; Aga, M.; Inoue, S.-i.; Ushio, S.; Iwaki, K.; Ikeda, M.; Kurimoto, M. Tryptanthrin inhibits interferon-gamma production by Peyer's patch lymphocytes derived from mice thathadbeen orally administered staphylococcal enterotoxin. *Biol. Pharm. Bull.* **2003**, *26*, 365−367.
(9) Honda, G.; Tabata, M.; Tsuda, M. The Antimicrobial Specificity of Tryptanthrin. *Planta Med.* **1979**, *37*, 172−174.
(10) Mitscher, L. A.; Baker, W. Tuberculosis: A search for novel therapy starting with natural Products. *Med. Res. Rev.* **1998**, *18*, 363−374.
(11) Yu, S.-t.; Chern, J.-w.; Chen, T.-m.; Chiu, Y.-f.; Chen, H.-t.; Chen, Y.-h. Cytotoxicity and reversal of multidrug resistance by tryptanthrin-derived indoloquinazolines. *Acta Pharmacol. Sin.* **2010**, *31*, 259−264.
(12) Hatakeyama, S.; Ochi, N.; Numata, H.; Takano, S. A new route to substituted 3-methoxycarbonyldihydropyrans; enantioselective synthesis of (−)-methyl elenolate. *J. Chem. Soc., Chem. Commun.* **1988**, 1202−1204.
(13) Green, G. R.; Evans, J. M.; Vong, A. K.; Katritzky, A. R.; Rees, C. W.; Scriven, E. F. *Comprehensive Heterocyclic Chemistry*; Pergamon Press: Oxford: U.K., 1995.
(14) Gadwood, R. C.; Kamdar, B. V.; Dubray, L. A. C.; Wolfe, M. L.; Smith, M. P.; Watt, W.; Mizsak, S. A.; Groppi, V. E. Synthesis and biological activity of spirocyclic benzopyran imidazolone potassium channel openers. *J. Med. Chem.* **1993**, *36*, 1480−1487.
(15) Clapp, L. B. 1,2,4-Oxadiazoles. *Adv. Heterocycl. Chem.* **1976**, *20*, 65−116.
(16) Azizian, J.; Karimi, A. R.; Arefrad, H.; Mohammadi, A. A.; Mohammadizadeh, M. R. Synthesis of Some Novel γ-Spirolactones. *Monatsh. Chem.* **2004**, *135*, 729−733.
(17) Azizian, J.; Karimi, A. R.; Mohammadi, A. A. Synthesis of Some Novel γ- Spiroiminolactones from Reaction of Cyclohexyl Isocyanide and Dialkyl Acetylene Dicarboxylates with 1-Benzylisatin and Tryptanthrine. *Synth. Commun.* **2003**, *33*, 387−391.
(18) Azizian, J.; Madani, M.; Souzangarzadeh, S. One-Pot Synthesis of Novel Derivatives of Spiro-[6H-Indolo [2,1-b]Quinazoline-6,3′-[1,2,4]Oxadiazoline]. *Synth. Commun.* **2005**, *35*, 765−768.
(19) Azizian, J.; Mohammadizadeh, M. R.; Zomorodbakhsh, S.; Mohammadi, A. A.; Karimi, A. R. Microwave-assisted one-pot synthesis of some dicyano- methylene derivatives of indenoquinoxaline and tryptanthrin under solvent free conditions. *Arkivoc* **2007**, *2007*, 24−30.
(20) Maryam, B.; Maryam, F.; Hasaninejad, A.; Rakovský, E.; Babaei, S.; Maryamabadi, A.; Mohebbi, G. One-pot, four-component synthesis of spiroindoloquinazoline derivatives as phospholipase inhibitors. *Tetrahedron* **2017**, *73*, 5144−5152.
(21) Beyrati, M.; Hasaninejad, A. One-pot, three-component synthesis of spiroindoloquinazoline derivatives under solvent-free conditions using ammonium acetate as a dual activating catalyst. *Tetrahedron Lett.* **2017**, *58*, 1947−1951.
(22) Jeeva, S.; Muthu, S.; Thomas, R.; Raajaraman, B.; Mani, G.; Vinitha, G. Co-crystals of urea and hexanedioic acid with third-order nonlinear properties: An experimental and theoretical enquiry. *J. Mol. Struct.* **2020**, *1202*, 127237.
(23) Kerru, N.; Gummidi, L.; Bhaskaruni, S. V. H. S.; Maddila, S. N.; Singh, P.; Jonnalagadda, S. B. A comparison between observed and DFT calculations on structure of 5-(4-chlorophenyl)-2-amino-1,3,4-thiadiazole. *Sci. Rep.* **2019**, *9*, 19280.
(24) Frisch, M. J.; Trucks, G. W.; Schlegel, H. B.; Scuseria, G. E.; Robb, M. A.; Cheeseman, J. R.; Scalmani, G.; Barone, V.; Mennucci, B.; Petersson, G. A.; Nakatsuji, H.; Caricato, M.; Li, X.; Hratchian, H. P.; Izmaylov, A. F.; Bloino, J.; Zheng, G.; Sonnenberg, J. L.; Hada, M.; Ehara, M.; Toyota, K.; Fukuda, R.; Hasegawa, J.; Ishida, M.; Nakajima, T.; Honda, Y.; Kitao, O.; Nakai, H.; Vreven, T.; Montgomery, J. A. ., Jr.; Peralta, J. E.; Ogliaro, F.; Bearpark, M.; Heyd, J. J.; Brothers, E.; Kudin, K. N.; Staroverov, V. N.; Kobayashi, R.; Normand, J.; Raghavachari, K.; Rendell, A.; Burant, J. C.; Iyengar, S. S.; Tomasi, J.; Cossi, M.; Rega, N.; Millam, J. M.; Klene, M.; Knox, J. E.; Cross, J. B.; Bakken, V.; Adamo, C.; Jaramillo, J.; Gomperts, R.; Stratmann, R. E.; Yazyev, O.; Austin, A. J.; Cammi, R.; Pomelli, C.; Ochterski, J. W.; Martin, R. L.; Morokuma, K.; Zakrzewski, V.; Voth, G. A.; Salvador Dannenberg, J. J.; Dapprich, S.; Daniels, A. D.; Farkas, Ö.; Foresman, J. B.; Ortiz, J. V.; Cioslowski, J. *Gaussian 09*; Revision E.01; Gaussian, Inc.: Wallingford CT, 2009.Fox.
(25) CCDC 945362 **4c** contains the supplementary crystallographic data.
(26) Kuruvilla, T. K.; Prasana, J. C.; Muthu, S.; George, J.; Mathew, S. A. Quantum mechanical and spectroscopic (FT-IR, FT-Raman) study, NBO analysis, HOMO-LUMO, first order hyperpolarizability and molecular docking study of methyl[(3R)-3-(2-methylphenoxy)-3-phenylpropyl]amine by density functional method. *Spectrochim. Acta, Part A* **2018**, *188*, 382−393.
(27) Raajaraman, B.; Sheela, N. R.; Muthu, S. Spectroscopic, quantum computational and molecular docking studies on 1-phenylcyclopentane carboxylic acid. *Comput. Biol. Chem.* **2019**, *82*, 44−56.
(28) Hiremath, S. M.; Suvitha, A.; Patil, N. R.; Hiremath, C. S.; Khemalapure, S. S.; Pattanayak, S. K.; Negalurmath, V. S.; Obelannavar, K.; Armaković, S. J.; Armaković, S. Synthesis of 5- (5-methyl-benzofuran-3-ylmethyl)-3H- [1, 3, 4] oxadiazole-2-thione and investigation of its spectroscopic, reactivity, optoelectronic and drug-likeness properties by combined acomputational and experimental approach. *Spectrochim. Acta, Part A* **2018**, *205*, 95−110.

https://doi.org/10.1021/acsomega.1c06781
ACS Omega 2022, 7, 7874−7884